Physical Modelling in Geotechnics

Evaluation of end bearing capacity of embedded pile with inclined base plate by chamber test

M.J. Seo & J.S. Lee
School of Civil, Environmental and Architectural Engineering, Korea University, Seoul, Korea

K. Han
Lyles School of Civil Engineering, Purdue University, West Lafayette, Indiana, USA

ABSTRACT: The objective of this study is to investigate the end bearing capacity characteristics of piles with inclined base plates based on shear wave velocities. In this study, model piles with or without an inclined base plate are installed in a chamber to simulate the ground stress condition. Load tests are conducted on the model piles using a loading system, which consists of a hydraulic jack, hand-pump, and loadcell. In addition, the shear wave in the soils below the pile base is measured using bender elements during the load tests. The unit end bearing capacity and shear wave velocity of the pile with the inclined base plate are higher than those of the pile without the plate. Furthermore, the test results demonstrate a good correlation between the unit end bearing capacity and shear wave velocity, which is afforded by the horizontal effective stress of the soil below the pile base. This study shows that an inclined base plate may effectively improve the end bearing capacity of embedded piles.

Keywords: bender element, embedded pile, end bearing capacity, inclined base plate, shear wave velocity

1 INTRODUCTION

The embedded pile method, which is typically used in Korea, is illustrated in Fig. 1. First, a hole is bored with a casing and an auger to the desired depth (Figs. 1(a) and 1(b)). Subsequently, a cement paste is injected into the borehole through the hollow section of the auger, and the auger is pulled out (Fig. 1(c)). A precast pile is inserted into the borehole (Fig. 1(d)), and the casing is pulled out (Fig. 1(e)). Finally, the pile head is tapped using a drop hammer to fix the pile base into the ground (Fig. 1(f)).

During the installation of the embedded pile, soil disturbance occurs in the borehole, which decreases in the relative density of the soil (Reese and Touma, 1972). The loosened soil surrounding the pile base may cause significant settlement and unsatisfactory bearing capacity. Hence, the pile base should be sufficiently fixed to the ground.

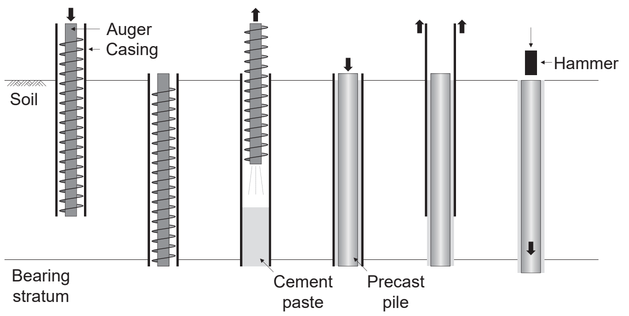

Fig. 1. Installation process of embedded pile: (a) excavating hole with auger and casing; (b) reaching bearing stratum; (c) injecting cement paste and uplifting auger; (d) inserting precast pile; (e) extracting casing; (f) final pile driving using drop hammer (modified from Han et al. (2019)).

Many studies have been conducted to improve the anchoring of embedded piles into soils. Seo et al. (2019) developed an embedded pile with the inclined base plate, which has a shape similar to a conical shell foundation. Seo et al. (2021) performed dynamic and static load tests to confirm the increase in the end bearing capacity by attaching an inclined base plate.

In this study, five different types of model piles were installed in a calibration chamber to examine the effect of the inclined base plate. Load tests were conducted on the model piles to evaluate the end bearing capacities based on the base shape. In addition, the shear waves were measured during the load test using bender elements installed beneath the pile base.

2 EXPERIMENTAL SETUP

A conventional pile with a flat base plate (Pile-C) and piles with base plates inclined at angles of 0°, 30°, 45°, and 60° (Pile-I00, I30, I45, and I60, respectively) were prepared to investigate the effect of the base shape on the end bearing capacity of the embedded pile. The diameters of the model pile and inclined base plate were 50 and 56 mm, respectively.

The model piles were installed in the calibration

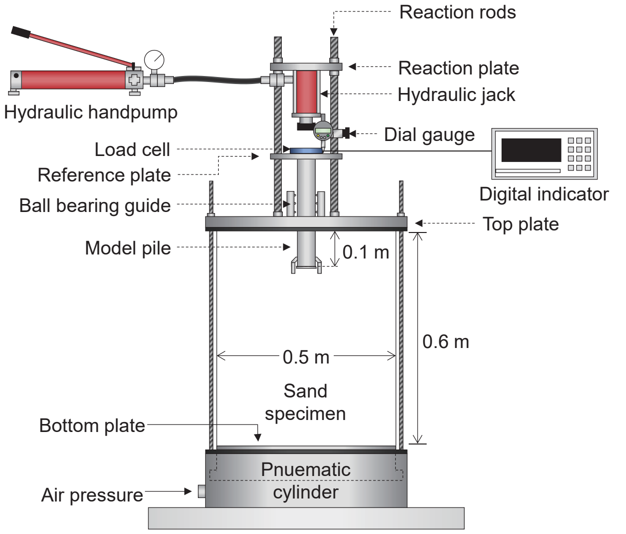

Fig. 2. Experimental setup with calibration chamber for performing load test.

chamber, as shown in Fig. 2. A pneumatic cylinder was installed at the bottom of the chamber to allow a vertical stress to be applied to the soil. The loading system, which consists of a hand pump and hydraulic jack, was installed below the reaction plate to allow a vertical load to be applied to the pile head. The load and settlement were monitored using a loadcell equipped with a digital indicator and digital dial gauge, respectively.

The measurement system used in this study is shown in Fig. 3. The base resistance was measured using strain gauges attached to the model pile. In addition, the bender elements were installed in the wedge-type frame to investigate the soil behavior beneath the pile base as shown in Fig. 3. The shape of the frame was obtained using field velocity probes developed by Lee et al. (2010) and Yoon and Lee (2010). A square wave with a voltage of 10 V was generated using a signal generator to measure the shear waves. The resonant frequency was estimated from the captured signal, which was measured using an oscilloscope. Subsequently, a single sinusoidal wave with an input frequency of the resonant frequency was generated.

Prior to the load test, a vertical stress of 100 kPa was applied for 24 h at the bottom of the calibration chamber, as shown in Fig. 2. After pressurization, equal load increments of 0.4 kN were applied to the pile head. Each load step was maintained for 5 min. The load test was terminated when the settlement exceeded 20% of the pile base diameter.

3 EXPERIMENTAL RESULTS

3.1 Load–settlement curves

The load–settlements estimated during the load tests are shown in Fig. 4. Fig. 4(a) shows the base resistance–settlement curves of the model piles with different base shapes. The base resistances of the piles

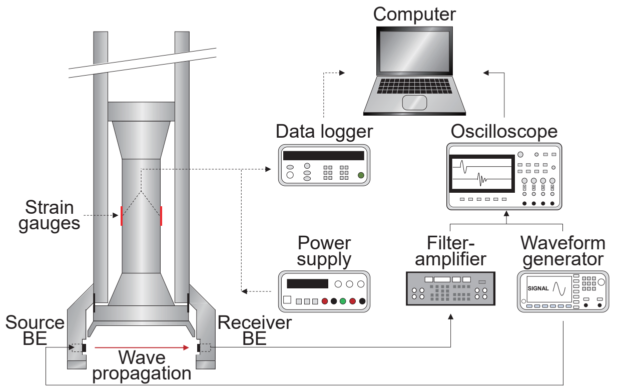

Fig. 3. Measurement system. Dashed and solid lines correspond to base resistance and shear wave measurement, respectively. BE denotes bender element.

with an inclined base plate are greater than those of the conventional pile for all settlements. For piles with inclined base plates, the base resistance increases with the inclination angle of the base plate. The unit base resistance–normalized settlement curves are plotted to disregard the effect of the increased projected area, as shown in Fig. 4(b). Fig. 4(b) shows that the unit base resistances of Pile-I45 and I60 are greater than those of Pile-C, I00, and I30. In other words, Pile-I45 and I60 demonstrate greater base resistance beyond the projected area increment.

3.2 Shear waves

The shear waves captured during the load tests are plotted to compare the soil behaviors based on the pile base shape, as shown in Fig. 5. Note that only the shear waves measured beneath Pile-C and I60 are plotted in Figs. 5(a) and 5(b), respectively, for clear comparison. Fig. 5 shows that the arrival time of the shear waves decreases as the base resistance increases. In addition, the shear waves for Pile-I60 (Fig. 5(b)) arrives earlier than those for Pile-C (Fig. 5(a)) for all load steps.

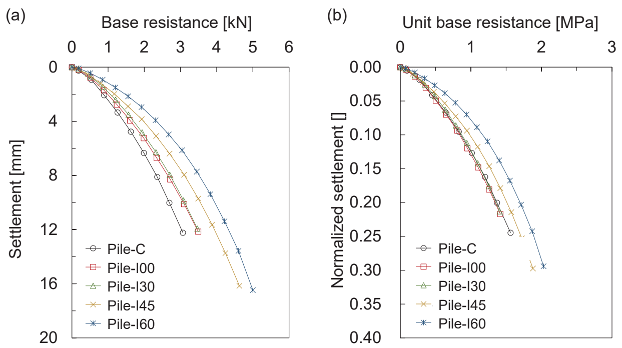

Fig. 4. Load–settlement curves based on base shape: (a) base resistance versus settlement; (b) unit base resistance versus normalized settlement.

Physical Modelling in Geotechnics
© 2022 KOREAN GEOTECHNICAL SOCIETY (KGS), Seoul, Korea, ISBN 978-89-952197-7-5

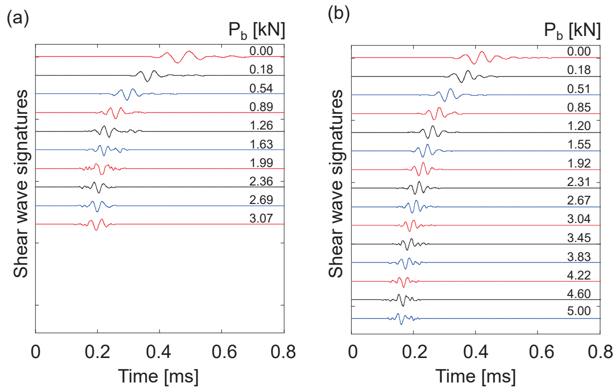

Fig. 5. Shear waves measured beneath pile base: (a) conventional pile; (b) pile with base plate inclined at angle of 60°. P_b denotes base resistance.

4 ANALYSES AND DISCUSSION

4.1 End bearing capacity

The end bearing capacities (Q_b) are evaluated as the base resistance at the base settlement of 10% of the pile base diameter based on the load–settlement curves, as shown in Fig. 4. The unit end bearing capacities (q_b) are evaluated for the removal of the increased projected area effect. The Q_b and q_b plotted in Fig. 6 were based on the pile base shape to compare the results as a function of the inclination angle of the base plate.

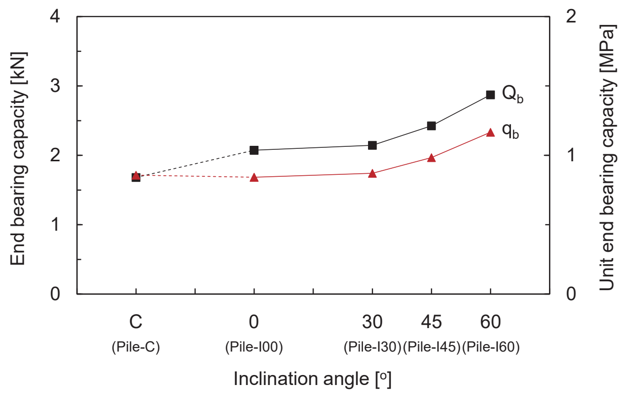

Fig. 6. End bearing capacities and unit end bearing capacities based on pile base shape.

Fig. 6 shows that the Q_b and q_b of Pile-I45 and I60 increases with the inclination angle. Fig. 6 indicates that the Q_b of Pile-I45 and I60 increases by 44.1% and 70.8%, respectively, compared with that of Pile-C. In addition, the q_b of Pile-I45 and I60 are higher than that of Pile-C by 14.9% and 19.9%, respectively, as shown in Fig. 6.

4.2 Shear wave velocity

The shear wave velocities estimated at the initial and failure stages (V_{so} and V_{sf}, respectively) are plotted in Fig. 7 based on the pile base shape. The V_{so} for Pile-I45 and I60 are 158.3 and 166.9 m/s, respectively, which are relatively high compared with those for Pile-C, I00, and I30, as shown in Fig. 7. The same tendency is observed in the shear wave velocity at the failure stage. The shear wave velocities are affected by the change in the horizontal stress of the soil, which is attributed to the packing type of granular materials (Santamarina et al., 2001). As the inclination angle of the base plate increases, more particles may be confined below the pile base. Therefore, the inter-particle contact size among the soils increases, and the horizontal stress beneath the pile base increases subsequently.

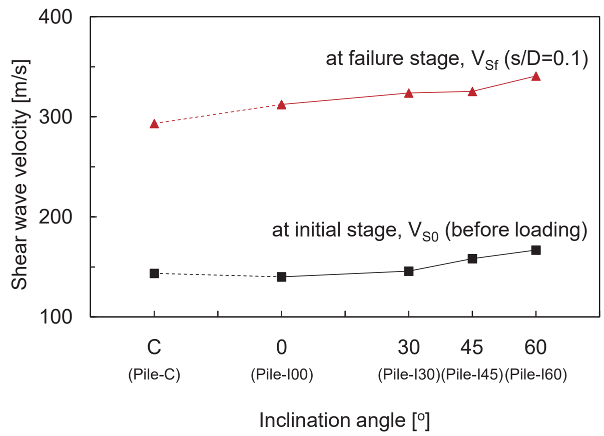

Fig. 7. Shar wave velocities at initial and failure stages based on pile base shape.

4.3 Effects of inclined base plate

The shear wave velocities against the base resistance or unit base resistance are plotted in Fig. 8. Figs. 8(a) and 8(b) show that the shear wave velocity increases with the base resistance and unit base resistance, respectively. Fig. 8(a) shows that the shear wave velocities at the same base resistance are almost identical regardless of the pile base shape, except at the initial stage. However, the shear wave velocities for the piles with inclined base plates at the same unit base resistance differ from those for the conventional pile, as depicted in Fig. 8(b). The difference may be caused by the size of the rupture surface or the confined zone formed below the pile base.

5 SUMMARY AND CONCLUSIONS

In this study, load tests were performed using model piles in the calibration chamber to investigate the effects of the inclined base plate on the end bearing capacity and the soil behavior below the embedded piles. The diameters of the pile and inclined base plate were 50 and 56 mm, respectively. A conventional pile with a flat base plate (Pile-C) and piles with base plates inclined at angles of 0°, 30°, 45°, and 60° (Pile-I00, I30, I45, and I60, respectively) were prepared to compare the base shapes. The model piles, which were equipped with strain gauges and bender elements, were installed to measure the shear waves during the load tests. Load tests were conducted until the base settlement exceeded 20%

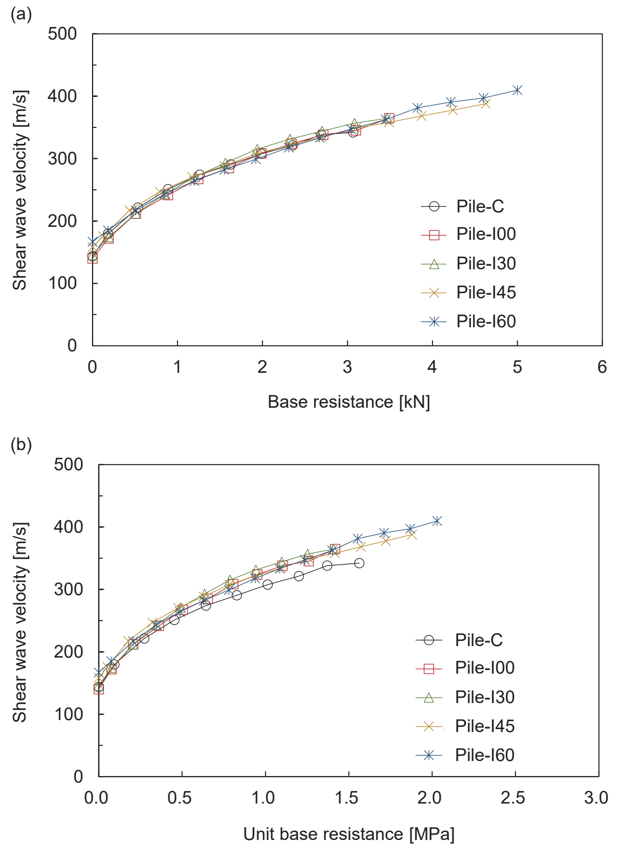

Fig. 8. Shear wave velocities versus: (a) base resistances; (b) unit base resistances.

of the pile base diameter after a vertical stress of 100 kPa was applied for 24 h. The load−settlement curves were obtained from the base load and settlement measured using strain gauges and a dial gauge. The end bearing capacities and unit end bearing capacities are evaluated using the base resistances at a base settlement of 10% of the pile base diameter. In addition, the shear wave velocities are evaluated using bender elements to investigate the soil behavior below the pile bases.

The end bearing capacities of the piles with inclined base plates are greater than that of the conventional pile. The end bearing capacity increases with the inclination angle of the base plate. The unit end bearing capacities, which are considered for the removal of the increased projected area, are greater for Pile-I45 and I60 than for Pile-C, I00, and I60. In addition, the shear wave velocities at the initial and failure stages increase with the inclination angle of the base plate increases. A more inclined base plate may confine more soil particles below the pile base and restrict their horizontal movement. Consequently, the end bearing capacity is greater because of the higher horizontal effective stress.

ACKNOWLEDGEMENTS

This work was supported by the Korean Small Business Innovation Research Program grant funded by the Korea Land & Housing Corporation and the National Research Foundation of Korea (NRF) grant funded by the Korea government (MSIT) (No. NRF-2021R1A5A1032433).

REFERENCES

Han, K., Seo, M. J., Hong, W.-T., and Lee, J.-S. 2020. End-bearing capacity of embedded piles with inclined-base plate: Laboratory Model Tests. *Journal of Geotechnical and Geoenvironmental Engineering* 146(8): 04020063.

Lee, J.-S., Lee, C.-H., Yoon, H.-K., and Lee, W.-J. 2010. Penetration type field velocity probe for soft soils. *Journal of Geotechnical and Geoenvironmental Engineering* 136(1): 199-206.

Reese, L. C. and Touma, F. T. 1972. Load tests of instrumented drilled shafts constructed by the slurry displacement method. Texas: Center for Highway Research, The University of Texas at Austin.

Santamarina, J. C., Klein, K. A., and Fam, M. A. 2001. Soils and waves. New York: Wiley.

Seo, M., Han, K., Park, J.-B., and Lee, J.-S. 2019. Tip resistance characterization of embedded piles with inclined tip plates using dynamic pile tests. In: *Proceedings of the 16th Asian Regional Conference on Soil Mechanics and Geotechnical Engineering, 14-18 October 2019*. Taipei.

Seo, M. J., Han, K., Park, J.-B., Jeong, K.-H., and Lee, J.-S. 2021. End bearing capacity of embedded pile with inclined base plate: Field dynamic and static tests. *Geomechanics and Engineering* 26(3): 261-274.

Yoon, H.-K. and Lee, J.-S. 2010. Field velocity resistivity probe for estimating stiffness and void ratio. *Soil Dynamics and Earthquake Engineering* 30: 1540-1549.